5-2018

Phase Field Model of Thermally Induced Phase Separation (TIPS) for the Formation of Porous Polymer Membranes

Ashley Green
University of Arkansas, Fayetteville

Aria Green
University of Arkansas, Fayetteville

Phase Field Model of Thermally Induced Phase Separation (TIPS) for the Formation of Porous Polymer Membranes

By

Aria Green

University of Arkansas Department of Mechanical Engineering

For the completion of the Honors Thesis Requirement

Faculty Advisor: Dr. Paul Millett

Graduate Student Advisor: M. Rosario Cervellere

April 26, 2018

Abstract

Most membrane research and development has been done through experimental work, which can be costly and time consuming. An accurate computational model would greatly reduce the need for these experiments. The focus of the research presented in this paper is to create an accurate computational model for membrane formation using thermally induced phase separation (TIPS). A phase field model is employed to create this model including the Cahn Hilliard Equation and Flory Huggins Theory. This model produced computational results that correspond well with theoretical and experimental results. The model was then adapted to correspond to the PVDF/DPC polymer-solvent system by incorporating kinetics and thermodynamic considerations specific to the system.

Acknowledgements

I would like to thank Professor Paul Millett for letting me become a part of his research team. He was very helpful guiding me on this journey. In addition, I would like to thank Rosario Cervellere, my graduate student mentor, for taking the time to work with me and to help me whenever I got stuck. I would also like to thank Dr. Ford and Dr. Qian for allowing me to attend group meetings and really making me feel like a part of the team.

I would like to thank the National Science Foundation Research Experience for Undergraduates Program for helping me get started with this research.

I would like to thank the MAST Center as well as 3M for their support of the project.

Finally, I would like to thank the University of Arkansas and the Honors College for giving me this opportunity. I have loved attending school and participating in the research community on campus, and thanks to the generous donors at the university, I have been able to attend college with minimal financial burden.

Contents

Table of Figures

1 Introduction

1.1 Motivation

The current market size of membrane technology is approximately $20 billion, and was expected to grow 8% between the years of 2015 and 2018 [1]. Decades of research have developed a thorough understanding of the thermodynamic and kinematic perspectives of membrane formation [1]. Most of this research has been done experimentally. An accurate computational model would allow manufacturers of membranes to run simulations instead of experiments in a lab. This ability would save manufactures time and money because they could observe the outcome of a system without purchasing the materials required or lab time to perform the physical experiment.

1.2 Objective

The objective of this research is to develop a computational model which, when given inputs specific to a polymer-solvent system, could mathematically determine the membrane formation. Analysis codes will also be used to determine the resulting membrane's average pore size, an important factor in determining whether the membrane is suitable for the desired application.

2 Background

2.1 Membrane Research

In recent years, the field of semi porous membrane technology has been rapidly growing [1]. One of the major applications of membranes is filtration. Membrane filtration can extend beyond the range of solid-liquid filtration to macromolecules and dissolved solutes, allowing for the separation of gas mixtures and multicomponent solutions [2]. Membrane technology has been

extended to fields such as desalination and waste water treatment, biotechnology, and environmental applications [1-2]. These filtration applications usually range from nanofiltration on the order of 0.001 μm to microfiltration on the order of 1-10 μm [1]. However, these applications can go as small as 0.0001 μm for reverse osmosis filtration and as large as 100 μm. These various filtration techniques can filter out algae and bacteria on the larger scale, macromolecules and organic compounds on the smaller scale, all the way down to salts such as calcium, magnesium, and sodium [1]. The current aim in membrane research is to prepare membranes with a morphology that is tailored for a specific application [2].

2.2 Manufacturing Membranes

Two of the most common manufacturing processes for these membranes are Solvent Induced Phase Separation (SIPS) and Thermally Induced Phase Separation (TIPS) [3]. The SIPS process for flat sheet membranes begins with the heating of the polymer to enable a homogenous solution when mixed with the solvent [4]. This polymer solution is then cast onto a chill roll, forming a flat sheet membrane [4]. The flat sheet is then submerged in a precipitation bath composed mostly of a non-solvent to the polymer [4]. The solvent diffuses into the precipitation bath and the non-solvent into the polymer solution, causing the polymer to re-solidify and the membrane to form [4]. Then, the flat sheet is washed, stretched, and prepared for packaging [4]. Figure 1 shows a diagram of this process.

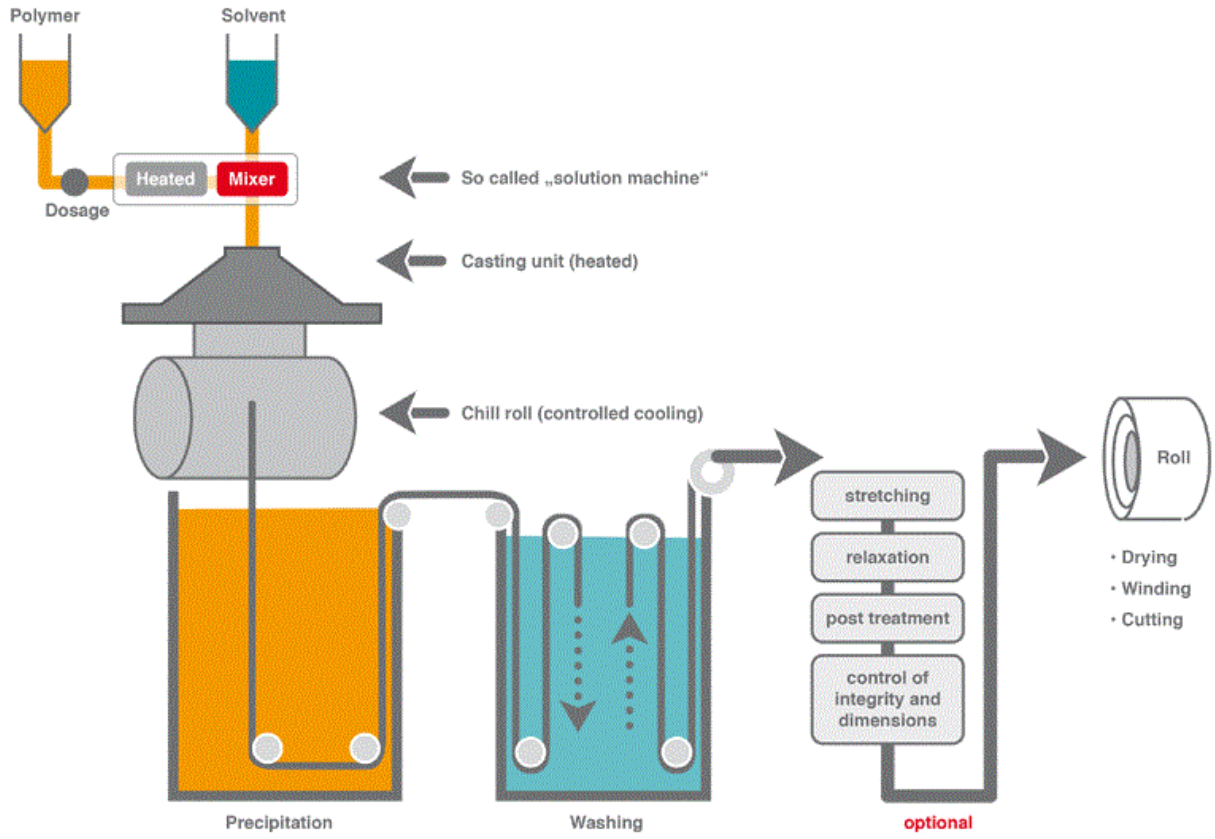

Figure 1. Manufacturing process using SIPS method [4]

The TIPS process is generally used whenever the polymer is not very compatible with the SIPS process [5]. The TIPS process, however, offers some advantages over the SIPS process such as simplicity, high reproducibility, and a low defect rate [1]. Figure 1 above shows the SIPS process, but has several steps that are replicated between the two processes. The polymer is first melted and pushed through an extruder where a mixer then combines the melted polymer with a solvent/non-solvent mixture to create a homogenous solution [5]. This solution is then extruded to form the desired shape, passed through an air gap, and then cooled either by quenching bath or a chill roll. This cooling is where the major difference between the SIPS process and the TIPS process comes in. This cooling drops the temperature of the solution below the spinodal line and causes phase separation to occur, forming polymer-rich and solvent-rich phases [5]. The polymer-

rich phase is then solidified in a precipitation bath and the membrane cleaned [5]. The compositions of the solvent-rich and polymer-rich phases can be determine using the phase diagram of the TIPS for specific polymer and solvent parameters. An example TIPS phase diagram can be seen in Figure 2. The TIPS process is the primary focus of the research presented here.

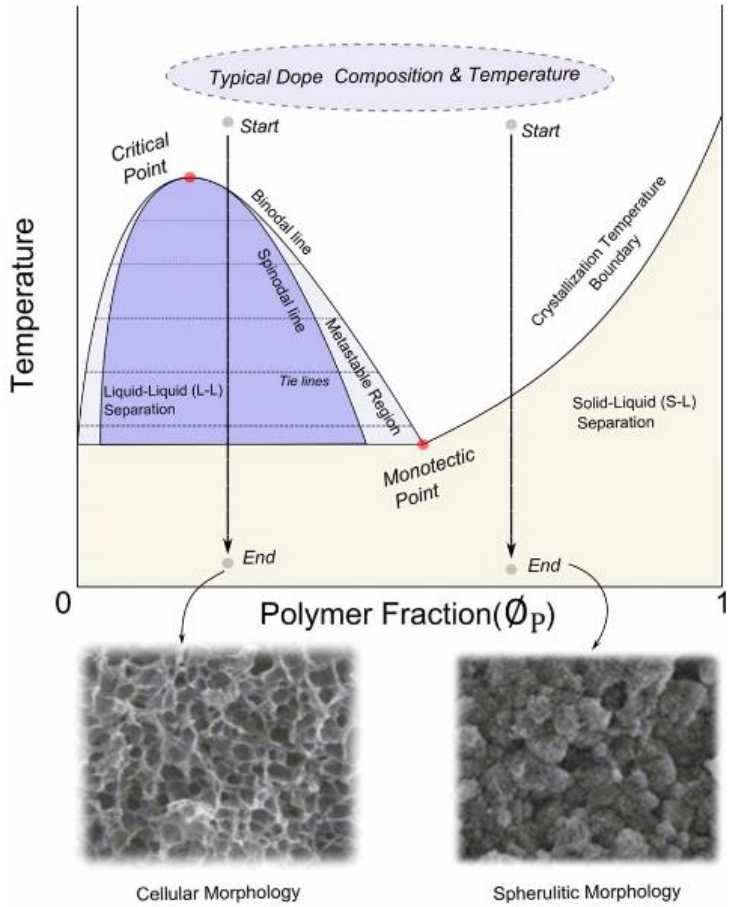

Figure 2. Phase diagram for typical TIPS process and resulting morphologies [1]

3 Methods

3.1 Phase-Field Methods

The model used to generate these simulations employs phase field methods. Phase-field methods are mesoscopic, thermodynamics-based, and describe the state of a system by functions of position and time [6]. These functions could be anything from specific properties of the system to abstract non-conserved quantities and are generally referred to as order parameters [6].

Concentration is a conserved order parameter since the total concentration is fixed and when the concentration of one species goes up in a region, the concentration of the other species goes down by the same amount [6].

3.2 Mathematical Modeling

The Cahn Hilliard equation is for conserved order parameters and can be written in terms of polymer concentration as

$$\frac{\partial \varphi_p}{\partial t} = \nabla \cdot M_p \nabla \mu$$

where φ_p is the polymer volume fraction, t is time, M_p is the concentration-dependent mobility, and μ is the chemical potential [6]. This equation presents an accurate model for the phase separation process. For the given system, the substitution

$$\mu = \frac{\partial \mathrm{F}}{\partial \varphi_p}$$

can be made, where F is the Gibb's free energy of mixing [6]. Gibb's free energy can be calculated using the Flory Huggins Theory

$$\mathrm{F} = k_b \mathrm{T} \left(\frac{\varphi_p \ln \varphi_p}{N_p} + \frac{\varphi_s}{N_s} \ln \varphi_s + \chi \varphi_p \varphi_s \right)$$

where k_b is the Boltzmann constant, T is the temperature in Kelvin, N_p and N_s are the degrees of polymerization for the polymer and solvent respectively, and φ_s is the solvent volume fraction [7]. The degrees of polymerization for the solvent can be set to one, providing further simplification. To simplify this equation, φ_s can be written in terms of φ_p as it is a conserved quantity [7].

$$\varphi_s + \varphi_p = 1$$

$$\therefore \varphi_s = 1 - \varphi_p$$

$$\mathrm{F} = k_b \mathrm{T}\left(\frac{\varphi_p \ln \varphi_p}{N_p} + (1-\varphi_p)\ln(1-\varphi_p) + \chi\varphi_p(1-\varphi_p)\right)$$

The derivative of the Flory Huggins Equation can be taken with respect to the polymer volume fraction to then be used in the Cahn Hilliard Equation. Below is this derivative in terms of φ_p.

$$\frac{\partial \mathrm{F}}{\partial \varphi_p} = k_b \mathrm{T}\left(\frac{\ln \varphi_p}{N_p} - \ln(1-\varphi_p) + \chi(1-2\varphi_p) + \frac{1}{N_p} - 1\right)$$

The Flory Huggins Interaction Parameter is found using the equation

$$\chi = \frac{\alpha}{T} + \beta$$

where α and β are constants obtained from a linear curve fit of experimentally determined solvent viscosity-temperature data [8].

3.3 Model One: PP and DPE

For the simulations ran, α and βwere assumed to be 714.0 and -1.235 respectively, and N_p equal to 150, corresponding to values found experimentally for the polymer-solvent system of polypropylene (PP) and diphenyl ether (DPE) [8]. This model employed the DeGennes model in order to calculate the mobility of the polymer [9].

$$M_p = 0.018\varphi_p^{7/4}$$

While this model is greatly simplified and is not temperature dependent, it is a good model to approximate the mobility without sacrificing speed of simulations and allowing for validation of other aspects of the model.

3.4 Model Two: PVDF and DPC

The model was revised to use values corresponding to the system of polyvinylidene fluoride (PVDF) and diphenyl carbonate (DPC), a more commonly used polymer-solvent system in membrane formation [10]. The constants α and β used in the calculation of the Flory Huggins

Interaction Parameter were revised to 425.0 and -0.338 respectively, corresponding to experimental data found for the system [10].

In model two, the model was expanded in order to include the Phillies model for polymer self-diffusion

$$D_s = D_0 \exp(-\alpha_1 c^{\nu})$$

where D_0 is the diffusion coefficient of an isolated macromolecule, c is the polymer weigh fraction (g/L), and α_1 and ν are scaling coefficients [11]. These scaling constants were assumed to be 0.2 and 0.4 respectively, corresponding to average values for polymer-solvent systems used in membrane formation processes [11]. This model can then be related to polymer mobility by [11]

$$M_p = \frac{D_s}{\frac{\partial^2 F_{mix}}{\partial \varphi^2}}$$

3.5 Simulation Process

The model begins by initializing the simulation field such that the solution is homogeneous. Once the simulation begins, the equations above govern the movement of the polymer and solvent as phase separation occurs. The simulations are run in dimensionless units of time and space in order to reduce computational time. The diffusion coefficient, which has units of area per time, allows for the relation of the simulation to a length and time scale. Using a known diffusion coefficient and choosing a desired length or time scale allows for the calculation of the other parameter.

A section of the code was implemented in order to gather data on the average diameter of the solvent-rich droplets. This data is important as the solvent-rich droplets become the pores whenever the polymer is solidified. These pore sizes are generally the primary factor that determine whether a membrane is appropriate for a specific application or not.

Simulations with this code were submitted to the Arkansas High Performance Computing Center (AHPCC). The output files were then analyzed in Paraview [12] to create 2D and 3D images depicting the concentration at each pixel. Videos were also created of the membrane formation over time.

4 Results

4.1 PP/DPE Model Results

The simulations in this report are isothermal TIPS simulations. When the simulation begins, the temperature immediately drops to the input temperature, causing phase separation to begin, and the simulation stays at that temperature until the end. Figure 3 shows the progression of a simulation with time as the mixture separates into polymer-rich and solvent-rich phases. The polymer-rich area is represented by the light, opaque color and the solvent-rich area is represented by the darker, transparent areas.

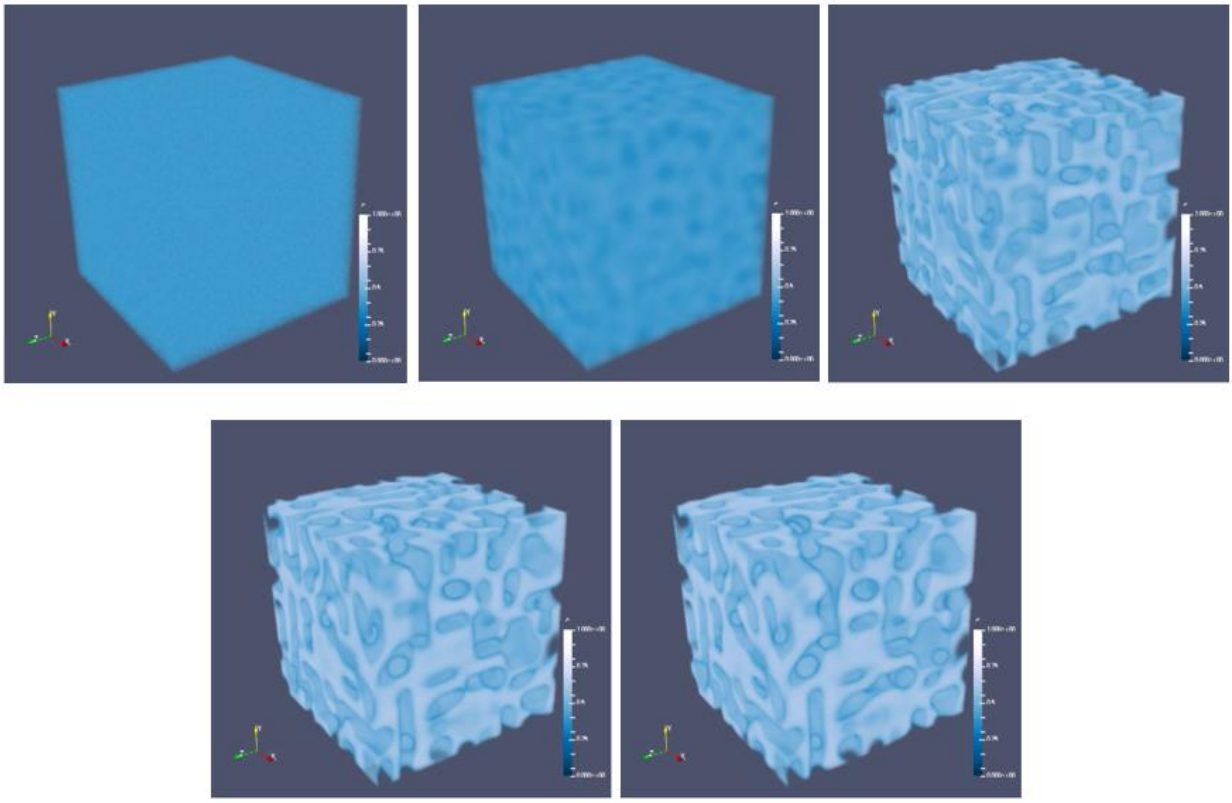

Figure 3. These are snapshots taken from one simulation at frames 1, 5, and 10 respectively for the top row and frames 15 and 20 respectively for bottom row [12]. This simulation is at 325K and a polymer volume fraction of 0.4.

The spinodal line was then graphed by setting the second derivative of the Flory Huggins Equation with respect to the polymer volume fraction equal to zero [7]. Simulations were ran at varying concentrations and temperatures. To compare these simulation results with theory, the images were placed over a graph of the spinodal line, as seen in Figure 5. The lighter colors represent polymer-rich areas and darker colors represent solvent-rich areas.

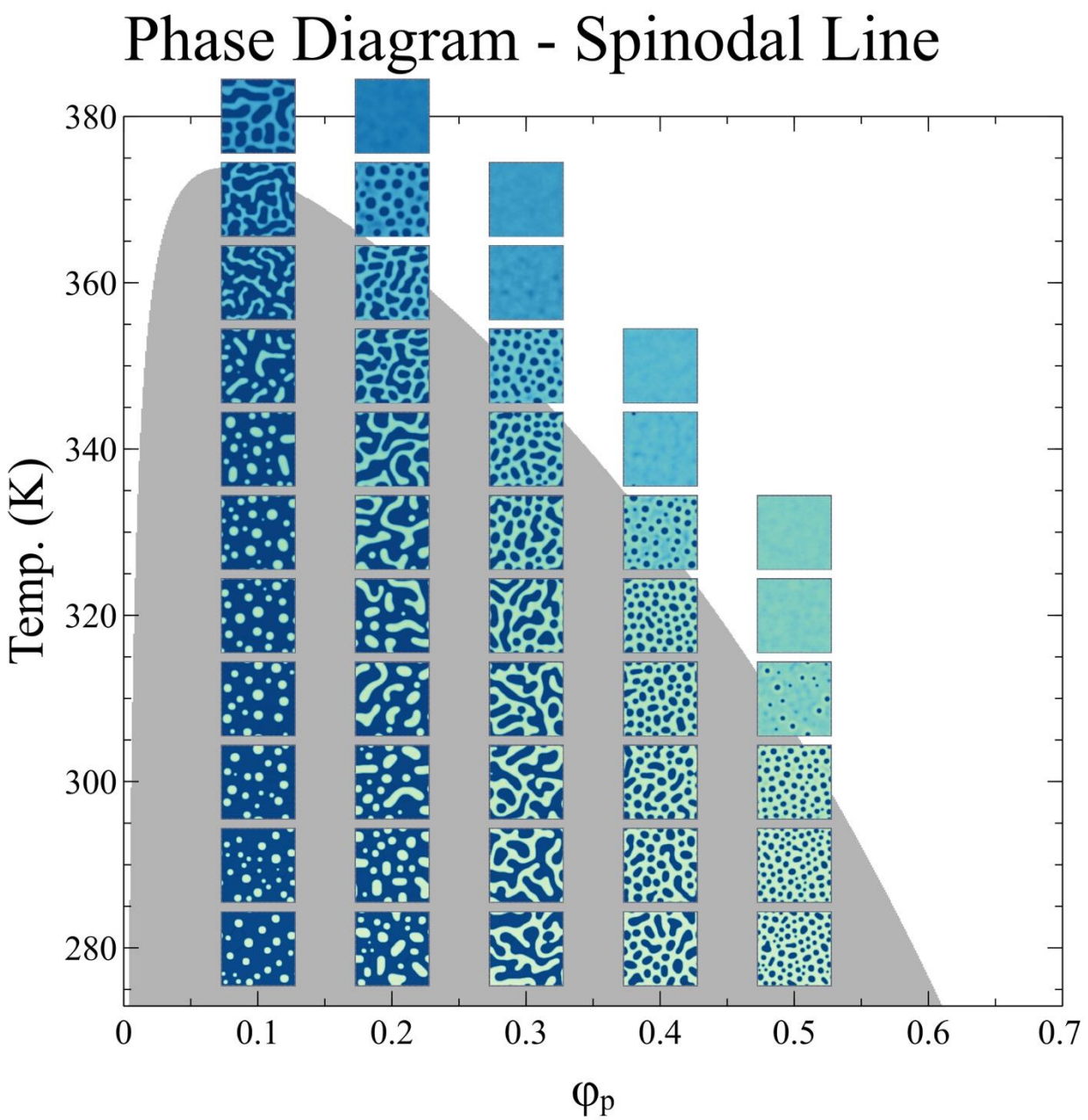

Figure 4. Simulation images are placed over a graph of the theoretical spinodal line to see correlation [12].

The data for the solvent-rich droplet diameters as the droplets develop over time can be seen in Figure 5. This can be compared to the visual results of simulations ran at the same temperatures and concentrations in Figure 6. Figures 7, 8, and 9 show the droplet diameters after 40,000 time

steps for different temperatures over five different runs per temperature. The error bars indicate the minimum and maximum values obtained within those five runs.

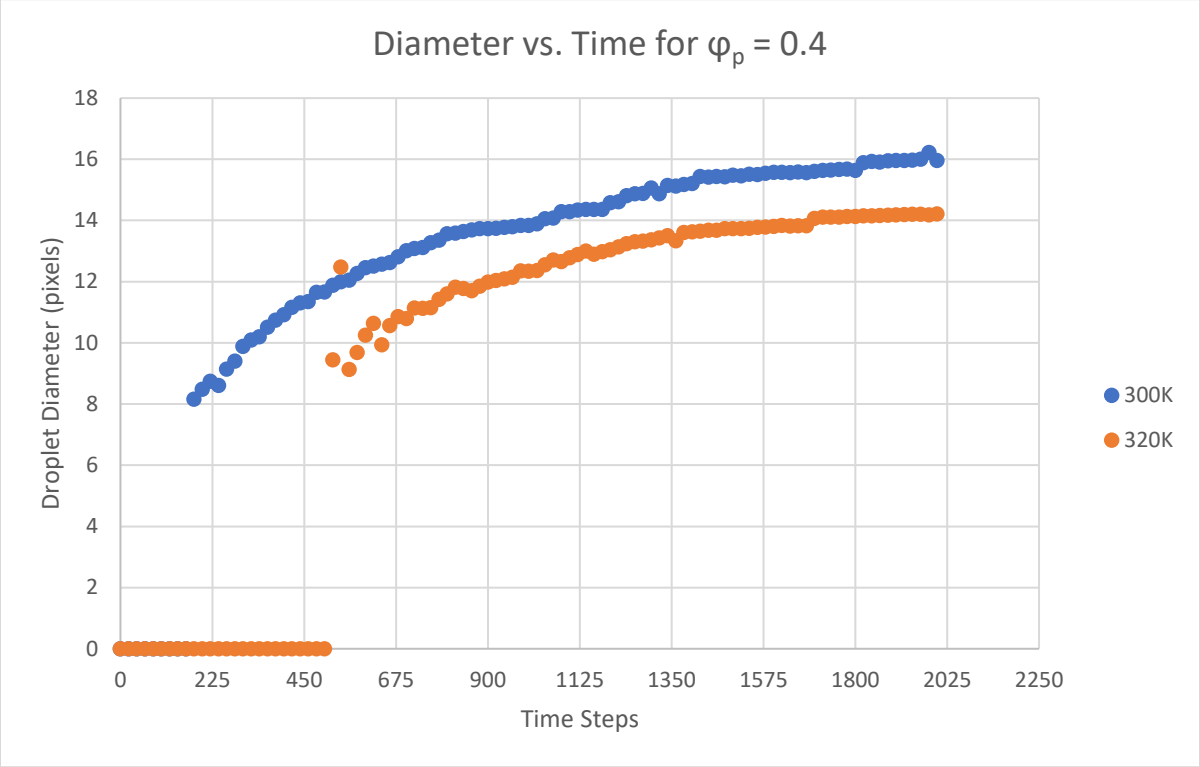

Figure 5. Droplet diameter over time at quenching temperatures 300K and 320K

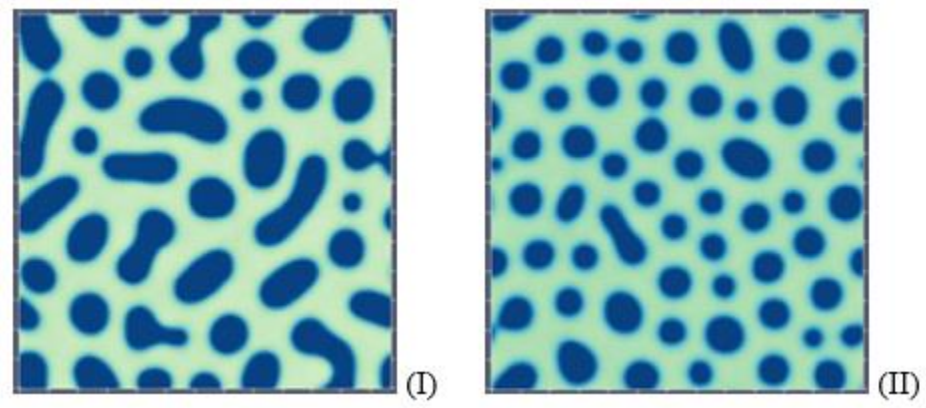

Figure 6. Simulation results for φ=0.4 and temperatures (I) 300K and (II) 320K [12]

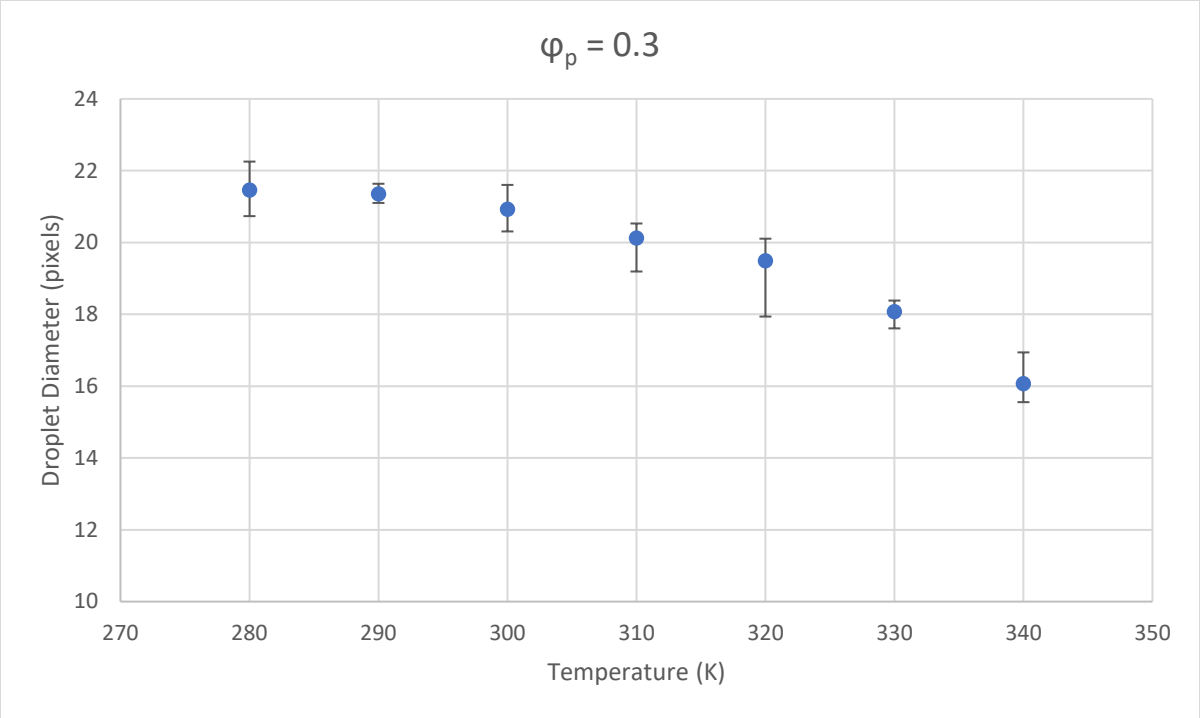

Figure 7. Droplet diameter averaged over five runs for each temperature with error bars for φ_p = 0.3

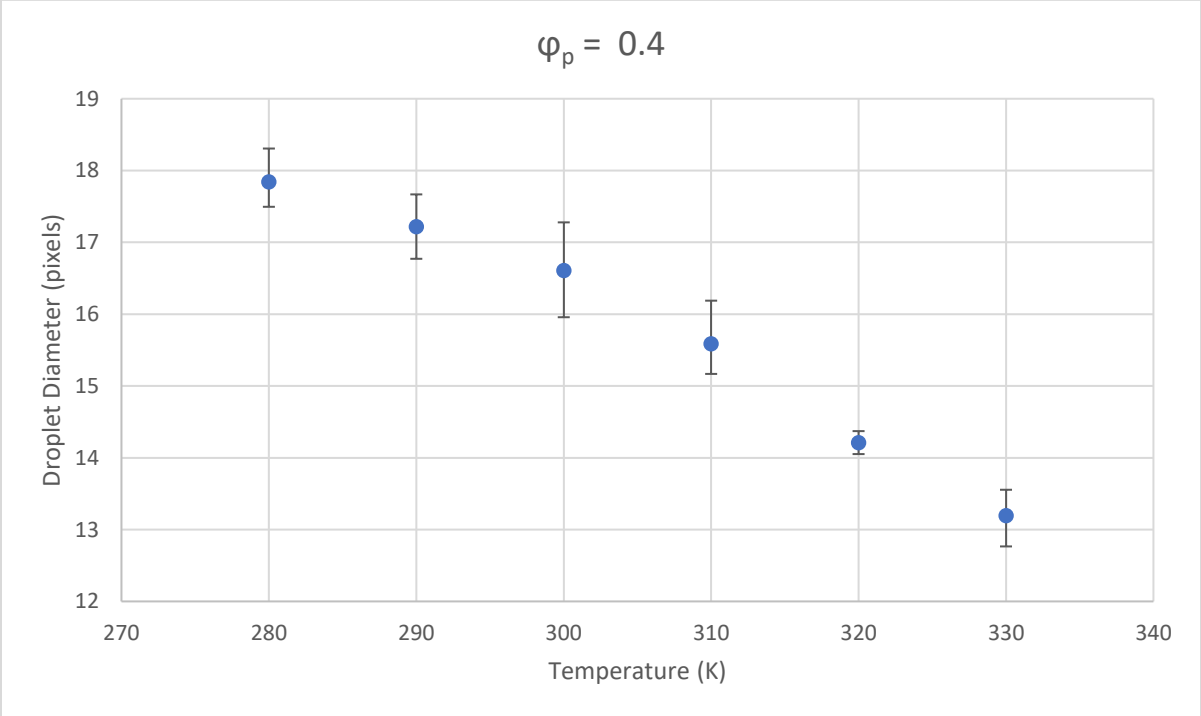

Figure 8. Droplet diameter averaged over five runs for each temperature with error bars for φ_p = 0.4

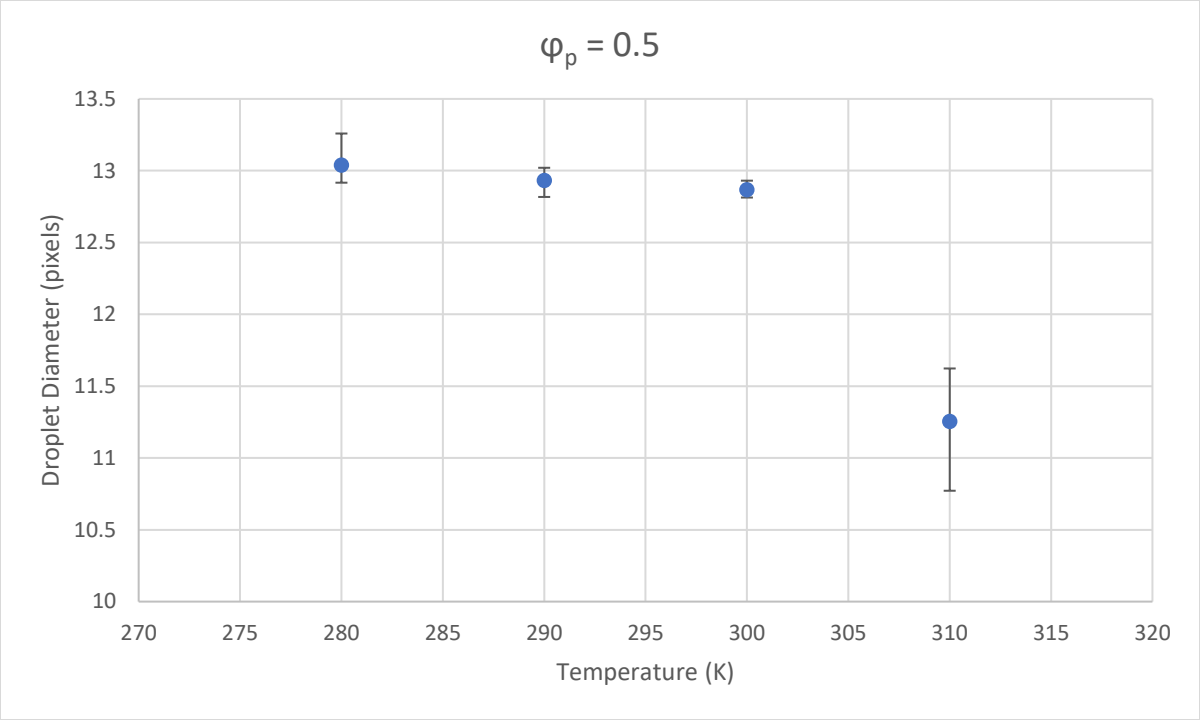

Figure 9. Droplet diameter averaged over five runs for each temperature with error bars for φ_p = 0.5

The diameter of the solvent-rich droplets can also be graphed as a function of concentration for a given temperature. Figure 10 and 11 show these graphs for 280K and 300K. The points represent the average droplet diameter of five runs, and the error bars show the minimum and maximum values obtained within those five runs per concentration. Figure 12 shows visual results for simulations ran at three different concentrations for 300K.

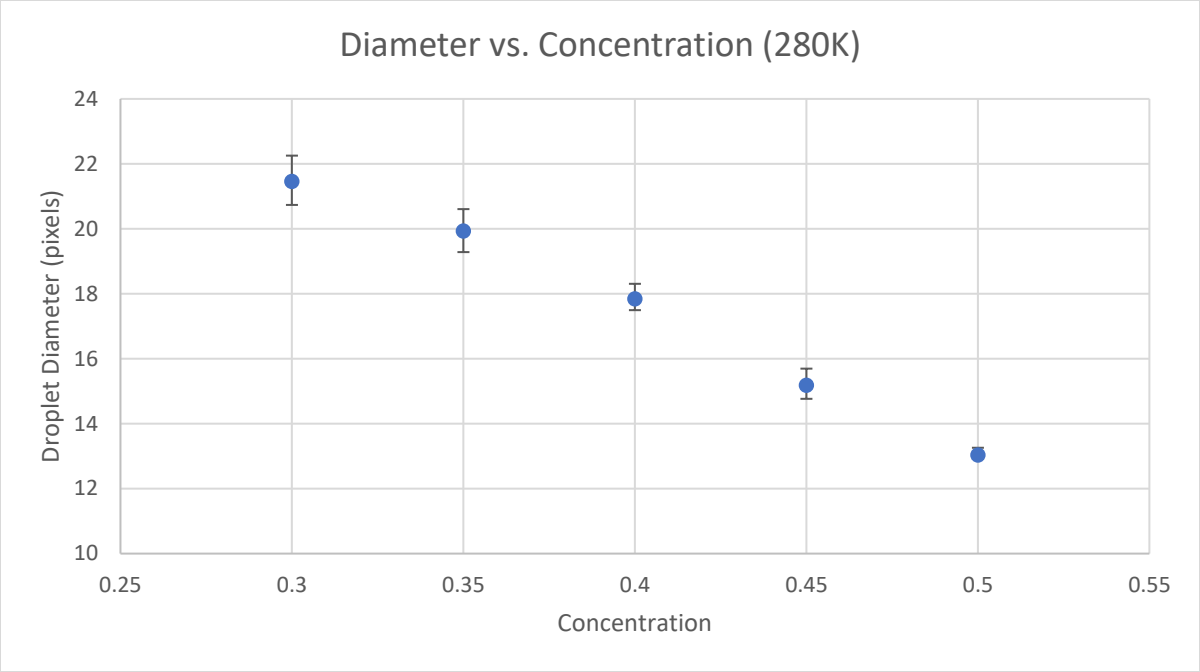

Figure 10. Droplet Diameter as a function of concentration for 280K

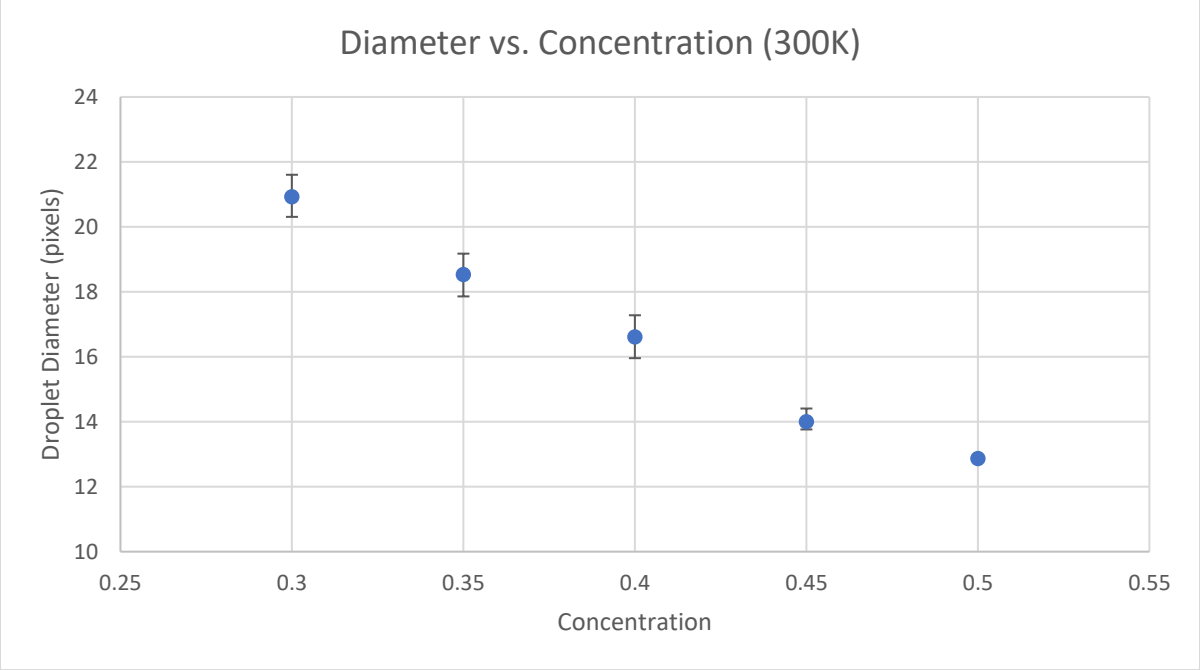

Figure 11. Droplet Diameter as a function of concentration for 300K

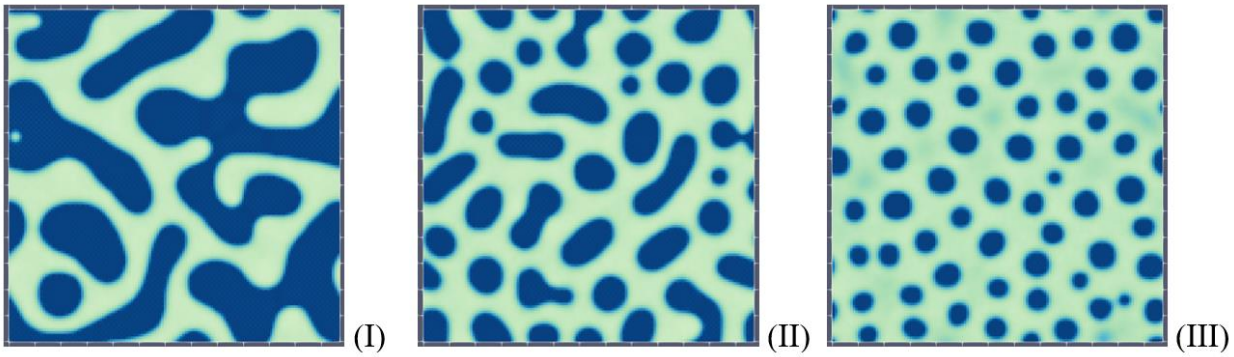

Figure 12. Final result of simulations ran at 300K for (I) $\varphi_p = 0.3$ (II) $\varphi_p = 0.4$ (III) $\varphi_p = 0.5$ [12]

4.2 PVDF/DPC Model Results

Multiple simulations were ran with the second model and the binodal and spinodal lines were graphed, following the same method of graphing as was used in model one with PP/DPE. These simulation results were then overlaid on the graph to see how well the simulation results corresponded to the theoretical results. These results can be seen below in Figure 13. The key to the side shows the varying color ranges and their corresponding polymer concentration values.

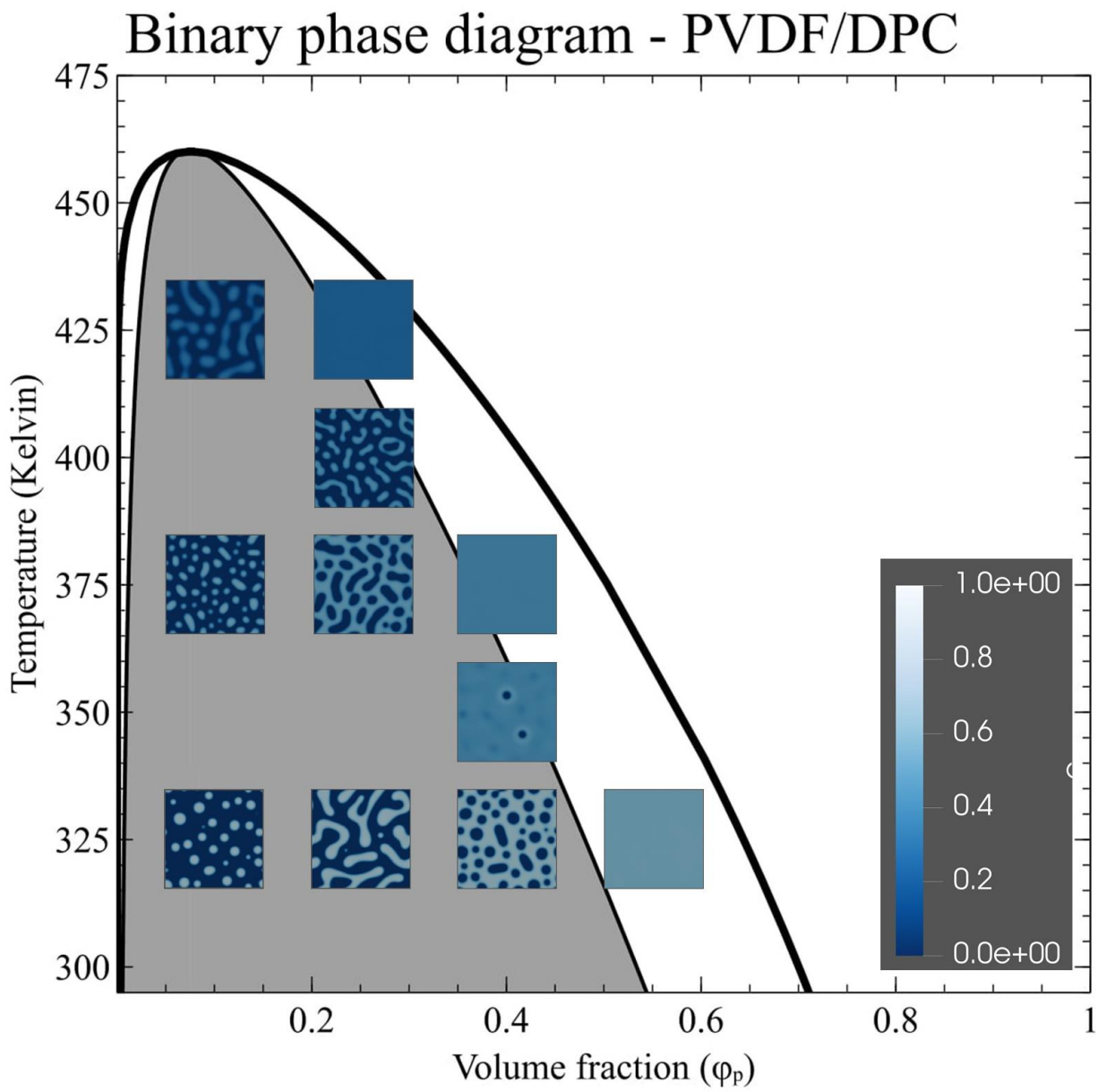

Figure 13. PVDF/DPC Phase Diagram with Simulation Results [12]

Once the model was verified, more simulations were ran in three dimensions. A newly developed script was used to determine the average distance between polymer regions, or pore diameter, as seen in Figure 14 below. Figure 15 shows simulation results using various polymer concentrations at 400K. These simulations visual correspond with the data plotting on the graph in Figure 14. Using an average diffusivity coefficient for PVDF/DPC system and time span of

simulations to be half a second in real time, the size of each pixel can be determined. The size of each pixel can then be extrapolated to determine the droplet size, as seen on the second axis of the graph.

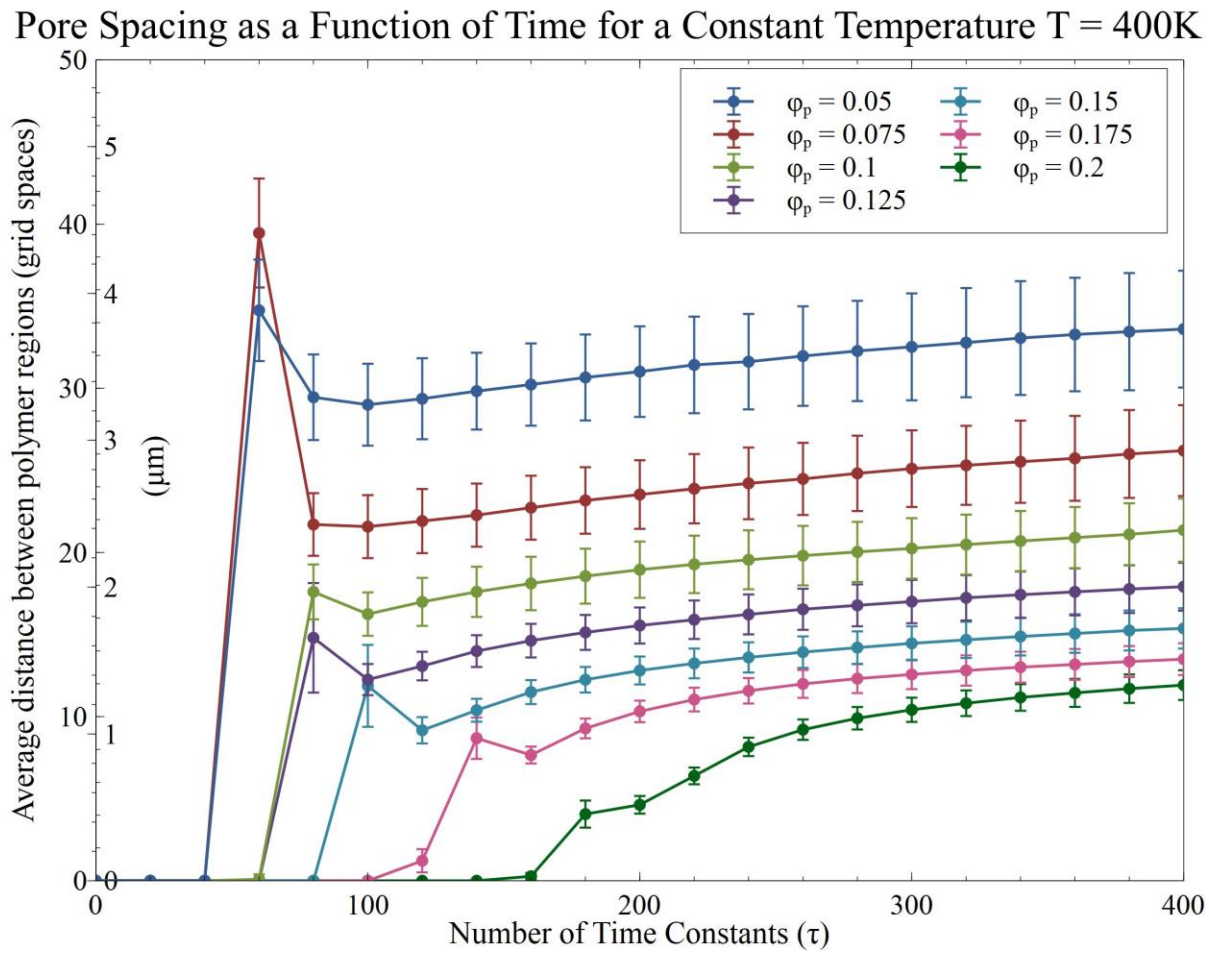

Figure 14. Pore Spacing as a Function of Time for Various Polymer Concentrations at 400K

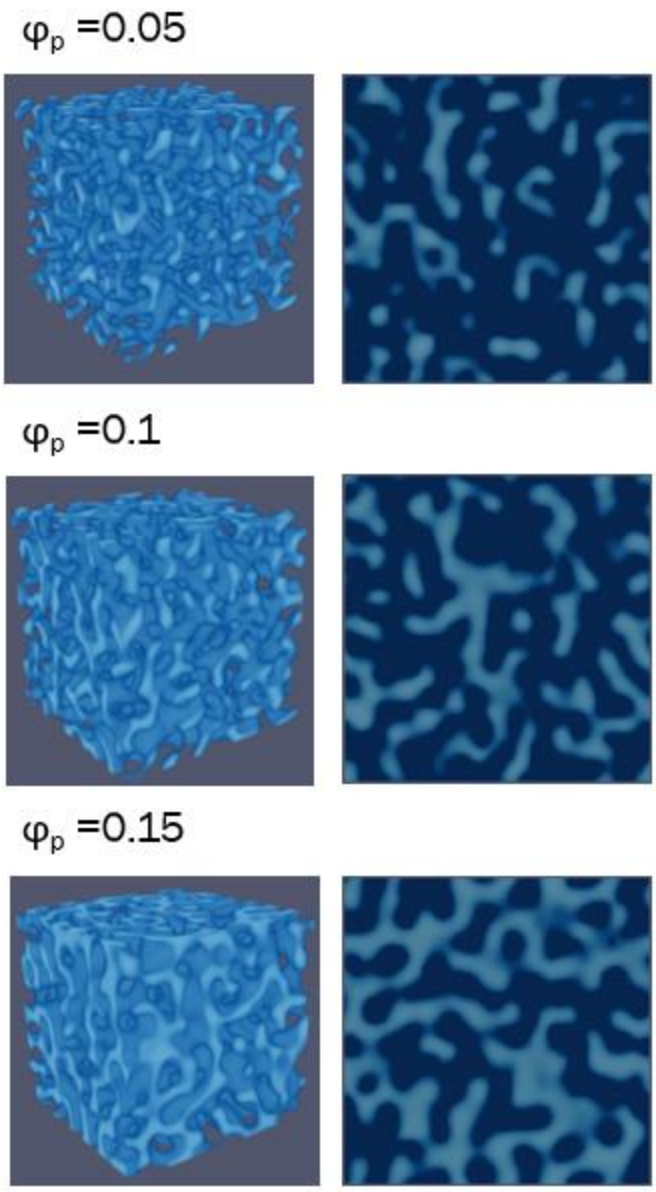

Figure 15. Simulation Results for Various Polymer Concentrations at 400K [12]

These simulations were also analyzed to see the relation between polymer concentration, temperature, and average distance between polymer regions using constant temperature lines. The resulting graph can be seen in Figure 16.

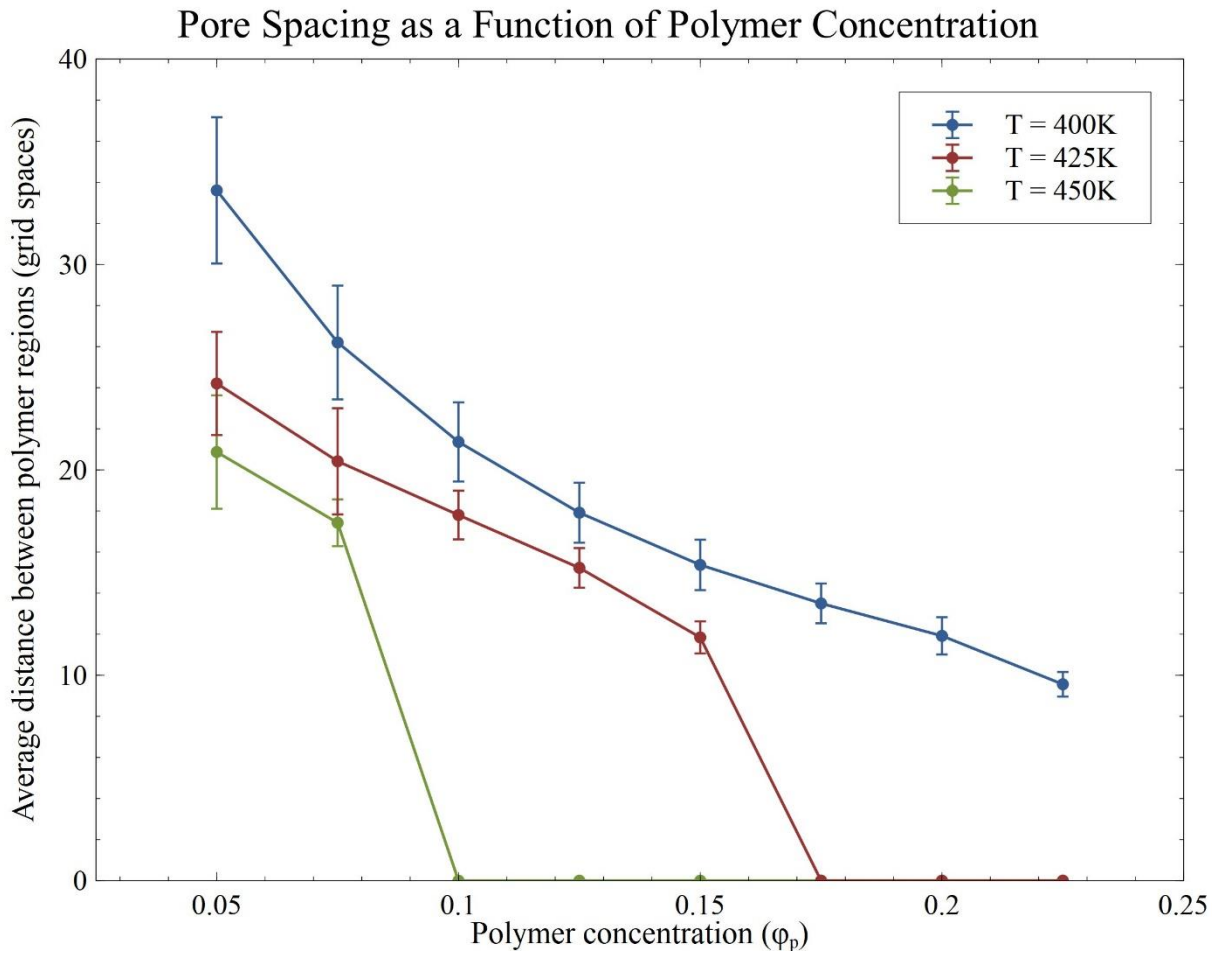

Figure 16. Pore Spacing as a Function of Polymer Concentration with Constant Temperature Lines

5 Conclusions

The simulation produced results that reflect the general trend of known experimental data. As seen in Figures 4 and 13, whenever the temperature rises above the spinodal line for a specific concentration, the solution does not phase separate. The simulation results achieved using the PVDF/DPC polymer-solvent system and the Phillies model corresponded closer to the system spinodal line than the PP/DPE model did with its respective spinodal line. Depending on the system and the polymer concentration, solvent-rich droplets, solvent-poor droplets, or a more bi-continuous mixture may occur. The droplet diameter increases over time, seeming to follow a

logarithmic growth. Increasing the simulation temperature and holding all other variables constant shifts the curve down, as seen in Figures 5 and 16. It can also be seen in these figures that at temperatures closer to the spinodal line produce droplet diameters that stay at zero for longer than lower temperatures. This is expected because at temperatures closer to the spinodal line, the demixing energy is lower and takes more time to overcome the nucleation barrier. The droplet diameter after the same number of time steps decreases as temperature increases with a constant concentration. The droplet diameter after the same number of time steps decreases as concentration increases.

6 Future Work

The model will need to be modified to include factors that can slightly modify the appearance of polymer-rich and solvent-rich areas such as viscoelastic effects. The model will also need to be adapted to better represent manufacturing processes of these membranes as opposed to idealistic scenarios. These manufacturing processes include the passing of the membrane through an air gap [5], which can cause some of the solvent to evaporate, and non-uniform temperature fields created by the cooling method of the membrane during formation. In addition, collaborations will need to be made with partners and interest parties in order to compare simulation results with experimental results, including the retrieval of more accurate, previously estimated, constants.

7 References

[1] Kim, Jeong F., Ji Hoon Kim, Young Moo Lee, and Enrico Drioli. "Thermally Induced Phase Separation and Electrospinning Methods for Emerging Membrane Application: A Review." *AlChE Journal* 62, no. 2 November 5, 2015. Accessed June 24, 2017.

[2] Guillen, Gregory R., Yinjin Pan, Minghua Li, and Eric M. V. Hoek. "Preparation and Characterization of Membranes Formed by Nonsolvent Induced Phase Separation: A Review." *ACS Publications*, March 8, 2011.

[3] "Manufacturing." Membrana. Accessed July 24, 2017. <http://www.membrana.com/technology/manufacturing>

[4] "SIPS" Membrana. Accessed July 24, 2017. <http://www.membrana.com/technology/manufacturing/sips>

[5] "TIPS" Membrana. Accessed July 24, 2017. <http://www.membrana.com/technology/manufacturing/tips>

[6] LeSar, Richard. *Introduction to Computational Materials Science: Fundamentals to Applications*. Cambridge: Cambridge University Press, 2013.

[7] Manias, Evangelos and Leszek A. Utracki. "Thermodynamics of Polymer Blends." Springer Science and Business Media, 2014, 197-99.

[8] He, Yan-Dong, Yuan-Hui Tang, and Xiao-Lin Wang. " Dissipative particle dynamics simulation on the membrane formation of polymer–diluent system via thermally induced phase separation." *Journal of Membrane Science*, November 12, 2010.

[9] de Gennes, P. G. "Dynamics of Fluctuations and Spinodal Decomposition in Polymer Blends." *The Journal of Chemical Physics 72*, no. 9, 1980, 4756-763.

[10] Tang, Yuan-hui, Yan-dong He, and Xiao-lin Wang. "Investigation on the membrane formation process of polymer–diluent system via thermally induced phase separation accompanied with mass transfer across the interface: Dissipative particle dynamics simulation and its experimental verification." *Journal of Membrane Science*, October 21, 2014.

[11] Phillies, George D. J. "Universal Scaling Equation for Self-diffusion by Macromolecules in Solution." *Macromolecules 19*, no. 9, 1986: 2367-376.

[12] Ayachit, Utkarsh, The ParaView Guide: A Parallel Visualization Application, Kitware, 2015, ISBN 978-1930934306